

1 Inhibitory properties of neomycin thin film formed on carbon steel in sulfuric acid solution.  
2 Electrochemical and AFM investigation  
3

4 Adriana Samide<sup>1,\*</sup>, Gabriela Eugenia Iacobescu<sup>2</sup>, Bogdan Tutunaru<sup>1</sup>, Roxana Grecu<sup>1</sup>,  
5 Cristian Tigae<sup>1</sup>, Cezar Spînu<sup>1</sup>

6  
7 <sup>1</sup>University of Craiova, Faculty of Sciences, Department of Chemistry, Calea Bucuresti 107i,  
8 Craiova, Romania; [tutunaruchim@yahoo.com](mailto:tutunaruchim@yahoo.com); [roxanamarius2008@yahoo.com](mailto:roxanamarius2008@yahoo.com);  
9 [ctigae@yahoo.com](mailto:ctigae@yahoo.com); [spinu\\_cezar@yahoo.com](mailto:spinu_cezar@yahoo.com)

10 <sup>2</sup>University of Craiova, Faculty of Sciences, Department of Physics, A.I. Cuza no. 1, Craiova,  
11 Romania; [gabrielaiacobescu@yahoo.com](mailto:gabrielaiacobescu@yahoo.com)

12 Correspondence: [samide\\_adriana@yahoo.com](mailto:samide_adriana@yahoo.com); Phone: +040251-597048.

## 14 Abstract

15 Our study aims to implement a strategy to reduce the carbon steel corrosion rate in sulfuric acid  
16 solution, using an expired drug with adsorption affinity on the metal surface. To investigate the  
17 corrosion protection efficiency of an environmental friendly inhibitor, namely neomycin sulfate  
18 (NMS), the electrochemical measurements were applied on carbon steel immersed in 1.0 M  
19  $\text{H}_2\text{SO}_4$  solution with and without NMS. The protective layer formed on the steel surface was  
20 studied by atomic force microscopy (AFM). The potentiodynamic polarization and  
21 electrochemical impedance spectroscopy (EIS) showed that the presence of the neomycin sulfate  
22 in acid solution leads to the decrease in corrosion current density ( $i_{\text{corr}}$ ) and the increase of  
23 polarization resistance ( $R_p$ ). The mixed mechanism between physical and chemical adsorption of  
24 NMS molecules on the steel surface was proposed according to the Langmuir adsorption  
25 isotherm. The Atomic Force Microscopy (AFM) indicated that the NMS molecules contributed to  
26 a protective layer formation by their adsorption on the steel surface. The AFM parameters such  
27 as: root-mean-square roughness ( $R_q$ ); average roughness ( $R_a$ ) and maximum peak to valley  
28 height ( $R_{p-v}$ ) revealed that in the presence of NMS a smoother surface of carbon steel was  
29 obtained, compared to the steel surface corroded in sulfuric acid blank solution.  
30

31  
32 **33 Keywords:** expired drug; corrosion inhibitor; potentiodynamic polarization; electrochemical  
34 impedance spectroscopy; AFM

## 35 36 1. Introduction

37 The different types of steel are widely utilized in many industrial fields due to their  
38 specific characteristics and properties. The lifetime of steel is influenced by the chemical or  
39 electrochemical reactions which take place at metallic material/environment interface. The  
40 carbon steel is used for the manufacturing of some industrial systems, such as pipes, pumps,  
41

43 turbine blades, water coolers and heaters. The contact with acidic/alkaline media leads to steel  
44 corrosion due to the oxidation reactions, its surface being partially or totally affected.

45 The corrosion control and prevention involve the use of effective methods to protect the  
46 metal surfaces. The change of the environment composition by the addition of some corrosion  
47 inhibitors represents an appropriate way to modify the contact interface between metal surface  
48 and electrolyte. The organic compounds act by adsorption on surface, forming protective layers  
49 with inhibitory properties against metal oxidation. The molecules of organic compounds contain  
50 oxygen, nitrogen and sulfur heteroatoms with high adsorption affinity on the metallic surfaces  
51 [1-8]. Thus, organic substances act by physical or chemical adsorption on the metal surface  
52 involving electrostatic interactions, physical or chemical bonds between unshared electron pairs  
53 of the heteroatoms and the *d*-vacant orbital of some metal atoms from surface [2-6].

54 Many types of compounds [2-13] such as drugs [2-9], plant extracts [10,13] and polymers  
55 [11,12] have been reported as efficient corrosion inhibitors that can contribute to the formation of  
56 protective layers on the carbon steel/stainless steel surfaces. The use of expired drugs in other  
57 activity fields could lead to the reduction of their disposal/destroying costs. A proper way is  
58 their reintegration into the chemical industry, as "Green Corrosion Inhibitors" for metallic  
59 materials [4-9, 14,15], being less toxic than others, having aqueous solubility and adsorption  
60 affinity for the metal surface and/or the capacity to form complexes with the metal ions released  
61 in solution during corrosion processes [4-8].

62 The weight loss method and electrochemical measurements coupled with different  
63 techniques such as scanning electron microscopy, X-ray photoelectron spectroscopy, UV-Vis  
64 spectrophotometry, high performance liquid chromatography and thermal analysis, have been  
65 used [2,4-8] to evaluate the inhibitory performance of some drugs for carbon steel corrosion in  
66 hydrochloric acid solution. Thus, for trimethoprim [2], quinine sulfate [4], aminophylline [5],  
67 sulfacetamide [6], sulfathiazole [7,8], the inhibition efficiency (*IE*) reached values between 80.0%  
68 and 93.0%, depending on their concentrations in studied environment. The XPS can accurately  
69 reveal the metal surface layer composition, both in the absence and presence of the inhibitor.  
70 From the high resolution XPS spectra, the binding energy can be determined and attributed to  
71 the corrosion products (oxides, hydroxides, oxy-hydroxides) and other bonds between  
72 atoms/heteroatoms from the molecules of the organic compounds. Thus, the change of surface  
73 layer composition due to the adsorption of some organic molecules can be highlighted [7,8].

74 Some expired drugs have also been used as corrosion inhibitors for other metals such as  
75 copper, aluminum and alloys. The metronidazole drug presented a high performance as  
76 corrosion inhibitor for copper in 1.0 M HCl solution [14]. Penicillins, cephalosporins,  
77 aminoglycosides, azoles and other drugs were the most studied compounds as corrosion  
78 inhibitors for aluminum and its alloys in various solutions [15, 16].

79 Recently, the use of neomycin as corrosion inhibitor for stainless steel in 2.0 M H<sub>2</sub>SO<sub>4</sub>  
80 solution [17], for carbon steel in 1.0 M HCl solution [18] and for mild steel in chloride  
81 environment [19] was reported. The inhibition efficiency of this drug was calculated according  
82 to the weight loss and electrochemical measurements. Raja *et al.* [17] proved that neomycin  
83 behaves as a corrosion inhibitor for 304L stainless steel in sulfuric acid solution, reaching an  
84 inhibition efficiency of about 89.0%, at its concentration of 3.0 mM, calculated from the mass loss  
85 method, the potentiodynamic polarization and the electrochemical impedance spectroscopy.

86 A.S. Fouda *et al.* [18] have studied the behaviour of the neomycin sulfate as corrosion inhibitor  
87 for carbon steel in 1.0 M HCl solution using chemical and electrochemical measurements,  
88 yielding from EIS, an inhibition efficiency value of 81.7%, the inhibitor concentration being of  
89  $15 \cdot 10^{-6}$  M. They conclude that the neomycin acted by adsorption, mainly due to electrostatic  
90 interactions between the inhibitor molecules and the steel surface. Chitra and Anand [19]  
91 calculated an inhibition efficiency of 75.1% for mild steel corrosion in 2.0 M KCl solution  
92 containing 0.5 mM neomycin using the mass loss method. The FTIR spectral study showed that  
93 the protective deposit consisted of a metal-neomycin complex. The IR adsorption peaks were  
94 attributed to some functional groups as (-OH) or bonds such as, C-H, C-N, C=C, C-O of the  
95 inhibitor molecules adsorbed on the steel surface [19].

96 In the present work, the effect of neomycin sulfate (NMS), with the molecular formula  
97  $C_{23}H_{46}N_6O_{13} \times H_2SO_4$ , on carbon steel corrosion inhibition in 1.0 M  $H_2SO_4$  was investigated using  
98 potentiodynamic polarization and electrochemical impedance spectroscopy (EIS). Moreover, the  
99 changes appeared in the surface morphology, and the protective layer characteristics formed by  
100 adsorption of NMS molecules were studied by Atomic Force Microscopy (AFM).

101  
102 **2. Experimental**

103  
104 *2.1. Materials*

105  
106 The carbon steel plates with an area of 1.0  $cm^2$ , and following composition (weight %):  
107 C=0.1%; Si=0.035%; Mn=0.4%; Cr=0.3%; Ni=0.3%; Fe in balance, were submitted to corrosion in  
108 1.0 M  $H_2SO_4$  solution. Before corrosion, the samples were mechanically polished with emery  
109 paper, ultrasonically cleaned, degreased with ethylic alcohol and dried in warm air. The  
110 corrosion tests were performed in 1.0 M  $H_2SO_4$  blank solution and 1.0 M  $H_2SO_4$  solution  
111 containing various neomycin concentrations: 0.3 mM; 0.5 mM; 0.7 mM; 0.9 mM. All reagents  
112 with adequate chemical purity were purchased from Sigma Aldrich.

113  
114 *2.2. Electrochemical measurements*

115  
116 Both potentiodynamic polarization and electrochemical impedance spectroscopy (EIS)  
117 were accomplished on carbon steel in 1.0 M  $H_2SO_4$  solution without and with various NMS  
118 concentrations using an electrochemical system VoltaLab with VoltaMaster 4 software. An open  
119 space electrochemical cell with three electrodes was used. The working electrode was  
120 manufactured from carbon steel plates with the area of 1.0  $cm^2$ . A foil of platinum (area of 1.0  
121  $cm^2$ ) and the Ag/AgCl electrode were used as auxiliary and reference electrodes, respectively.

122 The potentiodynamic polarization was conducted at the room temperature ( $23 \pm 1$  °C)  
123 with the potential scan rate of 1.0 mV  $s^{-1}$ , between -1000 mV and 100 mV, after 4.0 minutes of  
124 pre-polarization time of electrodes at open circuit. The potentiodynamic curves were processed  
125 as semi-log curves in the range of  $\pm 250$  mV with respect to the corrosion potential ( $E_{corr}$ ). The  
126 corrosion current density ( $i_{corr}$ ) was computed to the intersection of Tafel lines, at the corrosion  
127 potential. Also, to determine the polarization resistance ( $R_p$ ), the potentiodynamic polarization

128 curves were processed in a range close to the  $E_{corr}$  ( $\pm 20$  mV), where  $i$  vs.  $E$  plots represent straight  
129 lines with the slopes equal to  $1/R_p$ .

130 Before and after the potentiodynamic polarization, the UV-Vis spectrophotometric  
131 analysis of 1.0 M  $H_2SO_4$  solution containing 0.9 mM neomycin was carried out in the wavelength  
132 range from 800 nm to 200 nm. The UV-Vis spectrophotometer, Varian-Cary 50 type, with Cary  
133 WinUV software was used to obtain the analysis reports.

134 EIS was recorded as Nyquist diagrams in the frequency range of  $10^5$  Hz and  $10^{-1}$  Hz, with  
135 an amplitude signal of 10 mV, at the room temperature ( $23 \pm 1$  °C) after 4.0 minutes of relaxation  
136 time of the electrodes, at open circuit.

137

### 138 2.3. Atomic Force Microscopy (AFM) measurements

139

140 The surface morphologies of the carbon steel control sample and carbon steel corroded in  
141 1.0 M  $H_2SO_4$  blank solution and in 1.0 M  $H_2SO_4$  solution containing 0.9 mM NMS were studied  
142 by non-contact mode atomic force microscopy (NC-AFM, PARK XE-100 SPM system). The  
143 cantilever had a nominal length of 125 mm, a nominal force constant of 40 N/m, and oscillation  
144 frequencies in the range of 275–373 kHz. We used horizontal line by line flattening as  
145 planarization method. Average roughness ( $R_a$ ), root-mean-square (RMS) roughness ( $R_q$ ) and  
146 maximum peak to valley height ( $R_{p-v}$ ) of the surfaces were estimated over the areas of 45×45  
147  $\mu m^2$ .

148

## 149 3. Results and Discussion

150

### 151 3.1. Potentiodynamic polarization

152

153 The results of potentiodynamic polarization are presented in Figure 1. The  
154 potentiodynamic curves were processed as semi-log curves (Fig. 1a) from which the corrosion  
155 current density ( $i_{corr}$ ) was determined by applying the system of Tafel Equations (1 and 2) for  
156 anodic and cathodic processes. The polarization resistance ( $R_p$ ) was calculated from the linear  
157 shapes of polarization curves recorded close to  $E_{corr}$ , in the potential range of  $\pm 20$  mV (Fig. 1b),  
158 the corrosion current density ( $i_{corr}$ ) being computed by applying the Stern Geary Equation 3.

$$\eta = b_a \lg i - b_a \lg i_{cor} \quad (1)$$

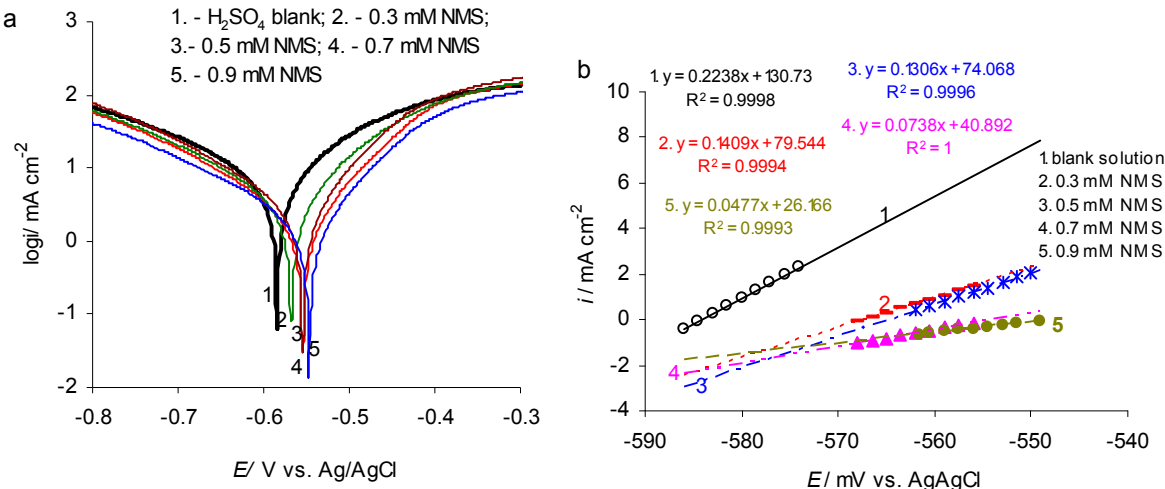
$$\eta = b_c \lg i_{cor} - b_c \lg i \quad (2)$$

$$i_{corr} = \frac{b_a \cdot b_c}{2,303(b_a + b_c)} \cdot \frac{1}{R_p} \quad (3)$$

161 where:  $\eta$  is over-voltage;  $b_a$  and  $b_c$  are Tafel anodic and cathodic slopes;  $i_{corr}$  and  $R_p$  are corrosion  
162 current density and polarization resistance, respectively.

163 From Fig. 1a, it can be seen that the addition of NMS leads to: (i) the shifting of curves  
164 to higher potential values for all NMS concentrations, which entails the increase of the corrosion  
165 potential ( $E_{corr}$ ) in proportion to the increase in drug concentration; (ii) the movement of the  
166 polarization curves in lower current areas highlights the decrease in corrosion current density  
167 ( $i_{corr}$ ) with the NMS concentration increase; (iii) the addition of NMS in 1.0 M  $H_2SO_4$ , solution

169 affects more the anodic process than the cathodic one and consequently, NMS acts as a mixed  
 170 inhibitor, predominantly anodic, indicating the occurrence of a protective film [20] on the carbon  
 171 steel surface that leads to the decrease of the corrosion current density.



172  
 173 **Figure 1.** The potentiodynamic polarization curves recorded for carbon steel corroded in 1.0 M  
 174  $\text{H}_2\text{SO}_4$ , in the absence and in the presence of NMS: a - Tafel diagram; b - linear diagram obtained  
 175 in the potential range of  $\pm 20$  mV around  $E_{\text{corr}}$ .

176  
 177 The main electrochemical parameters were calculated using VoltaMaster 4 software and  
 178 these are listed in Table 1. From the straight lines (Fig. 1b) drawn in the potential range of  $\pm 20$   
 179 mV, close to corresponding  $E_{\text{corr}}$ , the polarization resistance ( $R_p$ ) was determined according to  
 180 the Eq. 4 [14].  
 181

$$1/R_p = (di/dE)_{E \rightarrow E_{\text{corr}}} \quad (4)$$

182 where  $(di/dE)_{E \rightarrow E_{\text{corr}}}$  represents the slope of the straight lines shown in Fig. 1b.  
 183

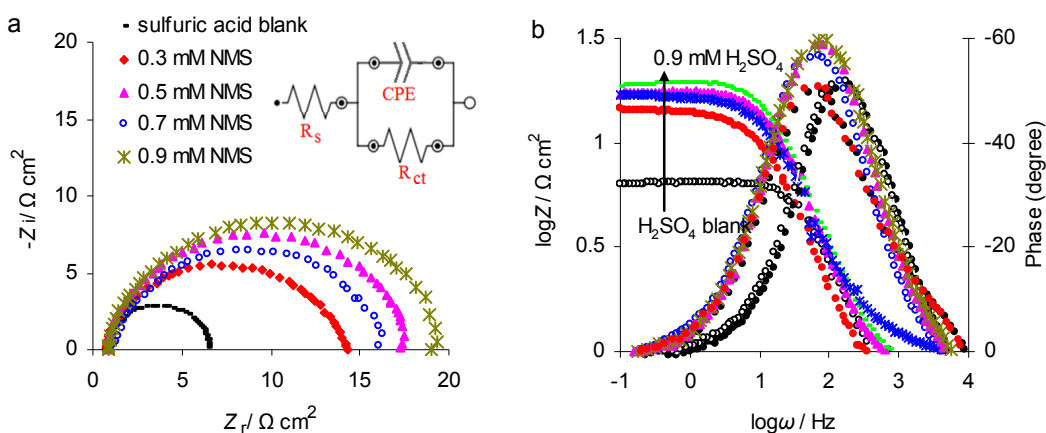
184 The slopes of straight lines were calculated by deriving the equations inserted in the  
 185 graph from Fig. 1b. A gradual increase of the polarization resistance is noticed, from  $4.4 \Omega \text{ cm}^2$   
 186 for the uninhibited solution to  $20.9 \Omega \text{ cm}^2$  for the solution containing 0.9 mM neomycin, thus  
 187 confirming the protective film formation [14] on the steel surface.  
 188

### 189 3.2. Electrochemical impedance spectroscopy (EIS)

190  
 191  
 192 Electrochemical impedance spectroscopy (EIS) was applied on carbon steel surface in 1.0  
 193 M  $\text{H}_2\text{SO}_4$  solution without and with NMS after 4.0 minutes relaxation time of the electrodes, at  
 194 open circuit. The Nyquist and Bode diagrams were recorded, as shown in Figure 2. The Nyquist  
 195 diagram (Fig. 2a) clearly shows that the increase of the NMS concentration leads to more  
 196 extensive capacitive loops recording and consequently, the charge-transfer resistance ( $R_{\text{ct}}$ )  
 197 increases [4,5,7]. The presence of neomycin in 1.0 M  $\text{H}_2\text{SO}_4$  solution leads to steel surface  
 198 changes due to the inhibitor adsorption and, thus, the polarization resistance ( $R_p$ ) increases with  
 199 the increase of the NMS concentration. The Bode diagram (Fig. 2b) shows that the impedance

200 response increases with the increase of the NMS concentration reaching a logarithmic value of  
 201 1.27, at an inhibitor concentration of 0.9 mM, significantly higher compared to that obtained for  
 202 the blank acidic solution, when the value of 0.9 was recorded for  $\log Z$ . Moreover, in the  
 203 presence of NMS, the phase angle maximum is shifted to lower frequencies compared to the  
 204 blank, varying from -51.63 degrees in the absence of NMS to -59.67 degrees in its presence.  
 205 Consequently, the presence of NMS leads to the appearance of a layer which interposes at the  
 206 metal/electrolyte interface, reducing the corrosion rate of carbon steel in sulfuric acid solution.

207 As in other studies [21,22] for the fitting the experimental data, the Randles equivalent  
 208 circuit (inserted in Fig. 2a) was used, where charge-transfer resistance ( $R_{ct}$ ) is linked in parallel  
 209 position with constant phase element (CPE), both being connected in series with solution  
 210 resistance ( $R_s$ ).



211  
 212 **Figure 2.** Nyquist (a) and Bode (b) diagrams recorded for carbon steel in 1.0 M  $\text{H}_2\text{SO}_4$  blank  
 213 solution and in 1.0 M  $\text{H}_2\text{SO}_4$  solution containing various NMS concentrations

214  
 215 The effect due to the carbon steel surface imperfections is reflected by the CPE [23]. The  
 216 CPE impedance ( $Z_{CPE}$ ) was calculated using the Equation 5 [23,24].

$$217 \quad Z_{CPE} = \frac{1}{T(j\omega)^n} \quad (5)$$

218 where:  $T$  is a proportional factor;  $j$  equals  $-1$ ;  $\omega$  represents the angular frequency;  $n$  is the phase  
 219 shift, between *zero* and *unity* related to the constant phase angle of the CPE. When  $n = 0$ ,  $Z_{CPE}$   
 220 corresponds to a resistance with  $R = T^{-1}$ ; if  $n = 1$ ,  $Z_{CPE}$  is a capacitance with  $C = T$ . When  $n$  is  
 221 closely near 1, the CPE obeys the capacitive behaviour, being assimilated with the double-layer  
 222 capacitance ( $C_{dl}$ ), as shown in Table 1.

223 Similar to potentiodynamic polarization, electrochemical parameters were calculated  
 224 using the VoltaMaster 4 software, and the results are presented in Table 1. Also, Table 1 shows  
 225 the inhibition efficiency ( $IE$ ) calculated as a function of ( $i_{corr}$ ) and ( $R_{ct}$ ), as shown the Equation 6  
 226 and 7 [20,23-25].

$$227 \quad IE = \frac{i_{corr}^o - i_{corr}}{i_{corr}^o} \times 100 \quad (6)$$

$$228 \quad IE = \frac{R_{ct} - R_{ct}^0}{R_{ct}^0} \times 100 \quad (7)$$

229 where:  $i_{corr}^0$  and  $R_{ct}^0$  are the corrosion current density and charge-transfer resistance, respectively  
 230 computed for the carbon steel corroded in 1.0 M  $H_2SO_4$  blank solution,  $i_{corr}$  and  $R_{ct}$  represent the  
 231 corrosion current density and charge-transfer resistance, respectively, computed for carbon steel  
 232 corroded in 1.0 M  $H_2SO_4$  solution containing various NMS concentrations.

233 In Table 1 the  $IE$  values obtained by averaging values computed from both  
 234 potentiodynamic polarization and EIS are presented.

235  
 236 **Table 1.** The effect of the NMS concentration on the electrochemical parameters obtained from  
 237 potentiodynamic polarization and EIS and its average inhibition efficiency ( $IE$ ) for carbon steel  
 238 corrosion in 1.0 M  $H_2SO_4$  solution at the room temperature

C-NMS/ mM	$E_{corr}/\text{mV}$ vs. Ag/AgCl	$i_{corr}/\mu\text{A cm}^{-2}$	$C_{dl}/\mu\text{F cm}^{-2}$	$n$	$R_{ct}/\Omega \text{ cm}^2$	IE/%		
						from Tafel	from EIS	average values
0	-584.5	1560	520	0.963	5.3	-	-	-
0.3	-568.0	690	290	0.981	14.4	55.8	63.2	59.5±3.5
0.5	-554.5	540	225	0.979	16.6	65.4	68.1	66.8±1.3
0.7	-554.0	460	197	0.975	17.2	70.5	69.2	69.9±0.7
0.9	-547.0	320	165	0.968	19.8	79.5	73.2	76.4±3.2

240  
 241 The experimental data listed in Table 1 shows that NMS behaves as corrosion inhibitor  
 242 for carbon steel, in 1.0 M  $H_2SO_4$  at the room temperature. The following arguments support this  
 243 statement: (i) the increase of the NMS concentration leads to  $i_{corr}$  breakdown while  $R_{ct}$  increases  
 244 and  $C_{dl}$  decreases; (ii)  $IE$  follows the same increasing trend as the inhibitor concentration; (iii) the  
 245 NMS inhibition action is due to the adsorption of its molecules on carbon steel surface,  
 246 contributing to formation of a surface protective layer [23-26].

247  
 248 *3.3. NMS adsorption mechanism*

249  
 250 The adsorption can be quantitatively expressed by applying adsorption isotherms. The  
 251 fitting of the degree of surface coverage ( $\theta$ ) values with the maximum regression coefficient ( $R^2$ )  
 252 enables the accurate determination of the adsorption-desorption equilibrium constant ( $K$ ) and  
 253 then the calculation of the standard adsorption free energy ( $\Delta G_{ads}^0$ ) [20-28].

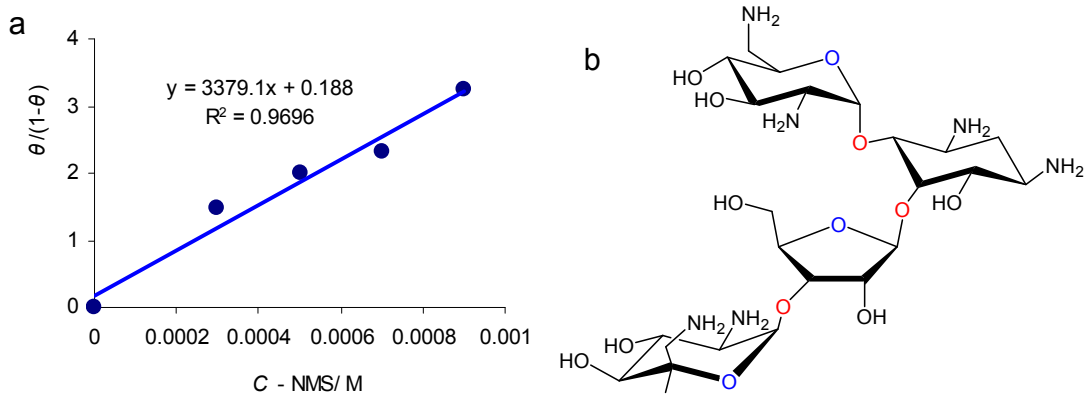
254 In our study, the experimental data were successfully fitted by applying the Langmuir  
 255 adsorption isotherm (Fig. 3a), its linearized form being expressed by the relation 8 [27].

256

$$\frac{\alpha}{1-\alpha} = K \cdot C \quad (8)$$

257 where  $C$  is the NMS concentration (M) in the bulk electrolyte;  $\theta$  is the average value of the  
 258 degree of surface coverage, being calculated as  $IE/100$ ;  $K$  is the adsorption-desorption  
 259 equilibrium constant.

260 By plotting  $\theta/(1-\theta)$  as a function of  $C$ , the straight line was obtained with the slope equal  
 261 to  $K$  (3379.1 L mol<sup>-1</sup>) and the  $R^2$  value of 0.97. Equation 9 was used to determine the standard  
 262 adsorption free energy ( $\Delta G^{\circ}_{ads}$ ) [26,27].



263  
 264 **Figure 3.** Langmuir diagram (a) corresponding to neomycin adsorption on carbon steel surface  
 265 in 1.0 M H<sub>2</sub>SO<sub>4</sub> inhibited solution and molecular structure of neomycin B (b)

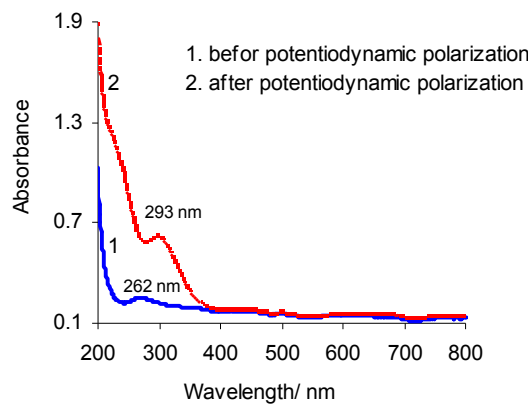
266  
 267  $\Delta G^{\circ}_{ads} = R \cdot T [\ln (1/55.5) - \ln K] \quad (9)$   
 268  
 269 where  $R$  is the universal constant of gases (8.31 J mol<sup>-1</sup> K<sup>-1</sup>),  $T$  is the temperature (298 K) and 55.5  
 270 is the value of the molar concentration of water in the solution.

271 The  $\Delta G^{\circ}_{ads}$  value of -30.06 kJ mol<sup>-1</sup> certifies a spontaneous moderate adsorption of NMS  
 272 molecules on carbon steel surface.

273 To appreciate the type of adsorption as physisorption or chemisorption the binding  
 274 energy ( $BE$ ) of the adsorbate to the substrate can be determined [5]. Thus, knowing that 1.0 kJ  
 275 mol<sup>-1</sup> is equal to 1.04· 10<sup>-2</sup> eV/molecule, it can be observed that the binding energy of neomycin  
 276 molecule reaches the value of 0.31 eV. This is higher than the typical binding energy of  
 277 physisorption that ranges between 0.01 eV and 0.1 eV, but less than that corresponding to  
 278 chemisorption when, usually, the binding energy varies from 1.0 eV to 10.0 eV. Consequently,  
 279 there is a synergism between the physical and chemical adsorption and consequently,  
 280 adsorption mixed mechanism of the neomycin molecules on the carbon steel surface takes place.  
 281 Based on the molecular structure of the inhibitor (Fig. 3b), it can be observed that the adsorption  
 282 of NMS molecules on carbon steel surface can be achieved by: (1) weak bonds between the  
 283 neomycin molecules and carbon steel surface suggesting physical adsorption which leaves intact  
 284 the chemical species; (2) stronger interaction between the neomycin molecules and the carbon  
 285 steel surface involving bonds between the unshared electron pairs from the oxygen and nitrogen  
 286 atoms and *d*-vacant orbital of iron from metal surface, indicating chemical adsorption; (3) also,

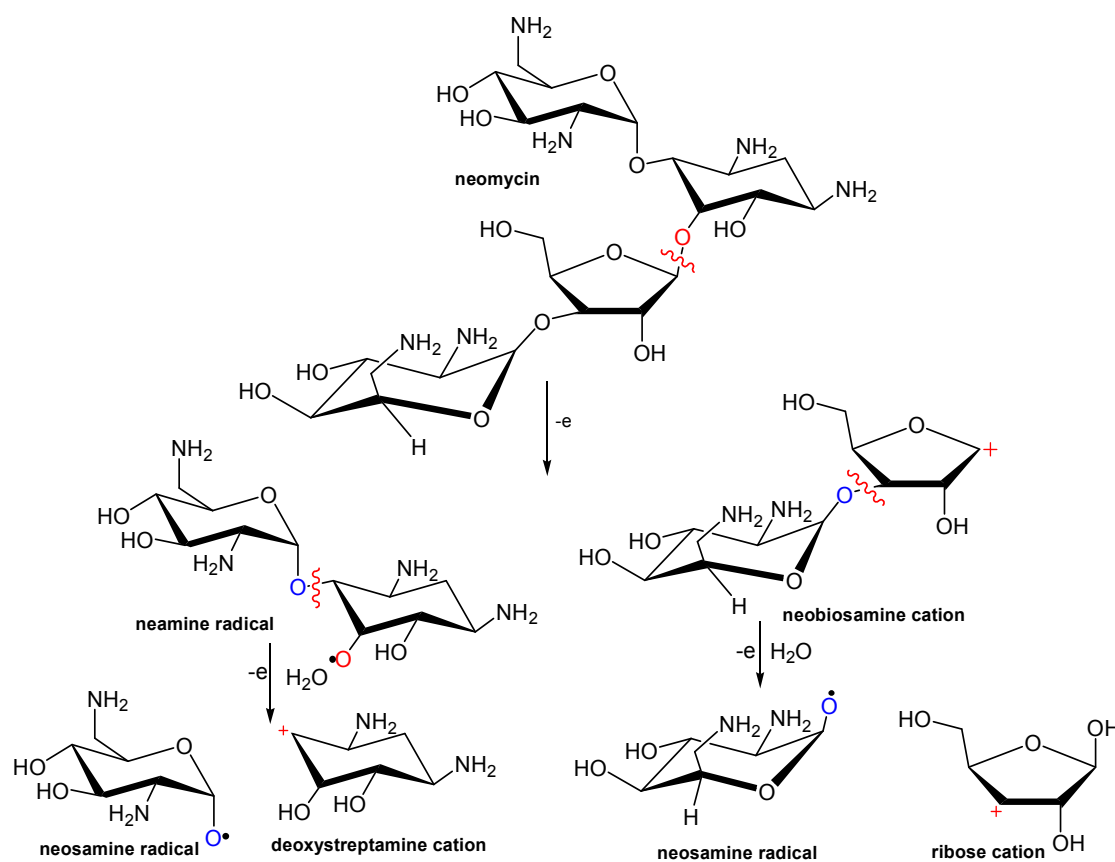
287 the complexes of neomycin-iron ions [19] can be adsorbed onto the steel surface through Van  
288 der Waals bonds [5].

289 Neomycin sulfate is a particular aminoglycoside antibiotic being the mixture of two  
290 stereoisomers as neomycin B (main product presented in Fig. 3b) and neomycin C, less than 3.0  
291 % [29,30]. Acid hydrolysis of neomycin B yields neamine and neobiosamine B; the hydrolysis of  
292 neomycin C leads to neamine and neobiosamine C [30]. Neobiosamine B and C are composed of  
293 D-ribose and neosamine B and C, respectively [30]. To elucidate the neomycin behavior, the UV-  
294 Vis spectrophotometry of 1.0 M H<sub>2</sub>SO<sub>4</sub> solution containing 0.9 mM neomycin was performed.  
295 The UV-Vis scans before and after potentiodynamic polarization are illustrated in Fig. 4.



296  
297 **Figure 4.** The UV-Vis scans of 1.0 M H<sub>2</sub>SO<sub>4</sub> solution containing 0.9 mM neomycin recorded  
298 before and after potentiodynamic polarization.

299  
300 Before the potentiodynamic polarization, the UV-Vis spectrum shows an absorption  
301 maximum centered around 262.0 nm; it starts at 312.0 nm and extends up to 235.0 nm. The UV-  
302 Vis spectrum of neomycin in bi-distilled water solvent showed an adsorption maximum at  
303 wavelength,  $\lambda_{\text{max}}$  of 304.8 nm [31]. Consequently, in 1.0 M H<sub>2</sub>SO<sub>4</sub> solution certain interferences  
304 with neomycin occur leading to the results above mentioned. After potentiodynamic  
305 polarization, a completely different spectrum was recorded. A peak highlighted at 293.0  
306 (beginning from 360.0 nm and ending to 260.0 nm) is followed by an extended loop from 267.0  
307 nm to 220.0 nm. These results suggest the environment composition changing, after  
308 potentiodynamic measurements, by the appearance of other chemical species formed by  
309 inhibitor decomposition reaction, interfering with neomycin around 293.0 nm. Thus, the  
310 concentration of neomycin decreases causing the alteration of its spectrum, but in the same time  
311 the absorbance increases due to new chemical species appearance. According to literature data,  
312 the main decomposition compounds consist of neamine and neobiosamine [30]. The neomycin B  
313 electrochemical decomposition mechanism is proposed, as shown in Scheme 1.

315  
316317 **Scheme 1.** The decomposition mechanism of neomycin B.

318

319 Neomycin exhibits relative stability during potentiodynamic polarization. In acidic  
 320 aqueous environments and high values of anode voltage, the etheric bridges between the  
 321 aminoglycoside cycles may be cleaved with the formation of neamine and neobiosamine as  
 322 main compounds and a mixture of other monocyclic species, leading to the composition  
 323 changing of corrosive environment (Scheme 1). Thus, during potentiodynamic measurements,  
 324 adsorbed molecules of neomycin and its electrochemical degradation compounds can occur on  
 325 carbon steel surface, involving the composition modification of the surface upper-layer.

326 The action mechanism of neomycin as corrosion inhibitor of carbon steel in 1.0 M H<sub>2</sub>SO<sub>4</sub>  
 327 solution is more complex than that reported for 304 stainless steel that involved physisorption  
 328 and other interactions [17], inhibitor performance being attributed to strong adsorption of  
 329 nitrogen atoms [17]. It is known that the 304 stainless steel has the composition and surface  
 330 characteristics different from those of carbon steel.

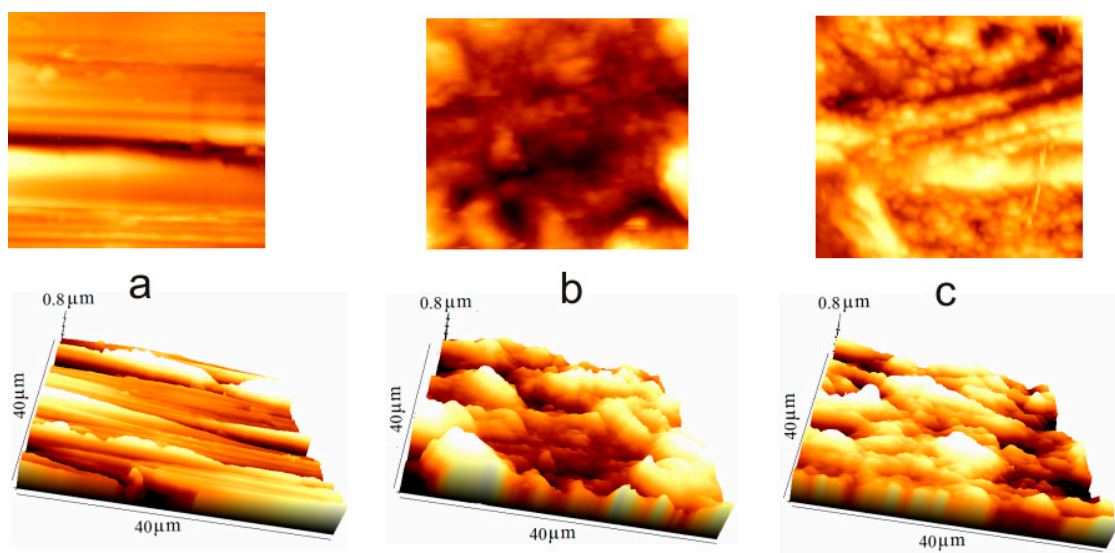
331

332 *3.4. Atomic Force Microscopy (AFM) technique*

333

334 The NMS addition in 1.0 M H<sub>2</sub>SO<sub>4</sub> solution modified the morphology and topography  
 335 of the carbon steel surface, as shown by AFM, based on the examination at nano-level of metal  
 336 surfaces [32], which is displayed in Figure 5. This figure illustrates the 2D and 3D images of

337 carbon steel surfaces, before and after potentiodynamic polarization in 1.0 M H<sub>2</sub>SO<sub>4</sub> solution  
 338 uninhibited and inhibited with 0.9 mM neomycin. Both 2D and 3D images highlight the major  
 339 change of surface morphology of carbon steel corroded in sulfuric acid without (Fig. 5b) and  
 340 with NMS (Fig. 5c) compared to that exhibited for the standard sample (Fig. 5a). Fig. 5a shows  
 341 the specific surface of the standard sample, which was initially subjected to a characteristic  
 342 mechanical processing.  
 343



344  
 345  
 346 **Figure 5.** 2D and 3D AFM images obtained for carbon steel surface: a - before corrosion (control  
 347 sample); b - after potentiodynamic polarization of carbon steel in 1.0 M H<sub>2</sub>SO<sub>4</sub> solution in the  
 348 absence of the inhibitor; c - after potentiodynamic polarization of carbon steel in 1.0 M H<sub>2</sub>SO<sub>4</sub>  
 349 solution containing 0.9 mM neomycin

350  
 351 In the inhibitor absence (Fig. 5b), the surface layer is uneven and strongly affected areas  
 352 that occurred during corrosion are highlighted. In contrast, the surface layer of carbon steel  
 353 corroded in the presence of NMS (Fig. 5c) is more uniform, suggesting that the neomycin  
 354 adsorbed molecules contributed to the surface protective layer formation.

355 The AFM parameters such as:  $R_q$  - Root-mean-square (RMS) roughness;  $R_a$  - Average  
 356 roughness;  $R_{p-v}$  - Maximum peak to valley height are presented in Table 2.

357 As expected, the smallest parameters were obtained for the standard sample. In the  
 358 absence of NMS, the higher values for  $R_a$ ,  $R_q$  and  $R_{p-v}$  were obtained, indicating that the surface  
 359 morphology and roughness changed [32,33]. In the presence of the NMS inhibitor, the values of  
 360 the AFM parameters decreased, indicating a smoother surface compared to that of carbon steel  
 361 corroded in blank solution, but higher than that of the standard sample.

362 Consequently, NMS behaves as corrosion inhibitor for carbon steel in 1.0 M H<sub>2</sub>SO<sub>4</sub>,  
 363 reaching an inhibition efficiency value of 76.4%, at a concentration of 0.9 mM. The interaction  
 364 process of neomycin molecules with the carbon steel surface takes place by a mixed mechanism  
 365 of spontaneous physical and chemical adsorption. The inhibitor electrochemical degradation  
 366 compounds contribute to the protective layer formation that restricts the corrosion processes.

367 It is noted that drugs have a significant inhibitory performance, most of them reaching  
 368 efficiency greater than 75.0%, depending on their concentration in the tested environment, type  
 369 of steel, electrolyte composition and pH, temperature, etc. [19, 27].  
 370

371 **Table 2.** AFM roughness parameters obtained for carbon steel uncorroded and corroded in  
 372 saline blank solution and in saline blank solution containing 0.5 mmol L<sup>-1</sup> FATTZ  
 373

375	Sample	$R_q$ / nm	$R_a$ /nm	$R_{p-v}$ /nm
377	Carbon steel, control sample	125.1	95.6	647.4
379	Carbon steel/1.0 M H <sub>2</sub> SO <sub>4</sub>	397.0	308.0	1634.0
380	Carbon steel/1.0 M H <sub>2</sub> SO <sub>4</sub> /0.9 mM NMS	170.1	127.1	896.6

382 In our previous studies, for the same type of carbon steel and under the same laboratory  
 383 conditions, we reported an inhibition efficiency of 93.6% for quinine sulfate, at 0.4 mM in 1.5 M  
 384 HCl solution [4], 92% for trimethoprim [2] and 87.3% for aminophylline [5], at 0.9 mM and 0.6  
 385 mM, respectively, in 1.0 M HCl solution. Moreover, the metronidazole inhibition performance in  
 386 1.0 M HCl solution was investigated for different substrates, when at an inhibitor concentration  
 387 of 0.8 mM, the inhibition efficiency reached 67.9% for 304L stainless steel [23], around 80.0% for  
 388 carbon steel [23] and copper [14] and 88.3% for aluminum [23].  
 389

390 The vanillin food additive tested as corrosion inhibitor for carbon steel in 10<sup>-3</sup> M HCl  
 391 solution containing 8.0 mM inhibitor reached an inhibition efficiency of 83.1% [34].

392 The amino-acids inhibition efficiency for the 316L stainless steel corrosion in 1.0 M H<sub>2</sub>SO<sub>4</sub>  
 393 containing 0.1 M inhibitor ranged as follows: glycine (84.2%)>valine (38.2%) >leucine (33.5%)  
 394 [35]. All these inhibitors acted by adsorption on substrates, blocking the surface active sites.  
 395

#### 396 4. Conclusions

397 Neomycin sulfate was investigated as inhibitor for the carbon steel corrosion in 1.0 M  
 398 H<sub>2</sub>SO<sub>4</sub> solution, using potentiodynamic polarization and electrochemical impedance  
 399 spectroscopy associated with AFM.

400 The electrochemical measurements showed that in the inhibitor presence the corrosion  
 401 current density decreased, while polarization resistance increased. Consequently, the inhibition  
 402 efficiency increased with the increase of the inhibitor concentration, reaching an average value  
 403 of 76.4%, at 0.9 mM neomycin concentration.

404 The experimental data were fitted according to the Langmuir adsorption isotherm, from  
 405 which the adsorption-desorption equilibrium constant ( $K$ ) value of 3379.1 L mol<sup>-1</sup> was  
 406 calculated. The standard adsorption free energy ( $\Delta G^{\circ}_{ads}$ ) of -30.06 kJ mol<sup>-1</sup> was obtained, and  
 407

409 consequently, a mixed mechanism for spontaneous adsorption of neomycin molecules was  
410 proposed as the synergism between physical and chemical adsorption, the first prevailing.

411 The surface protective layer composition mainly consists from neomycin and a mixture  
412 of its derivative compounds and complexes of inhibitor-iron ions, inclusively.

413 AFM confirmed that the neomycin adsorbed molecules on carbon steel surface  
414 contributed to the occurrence of a more uniform protective layer than that formed in the absence  
415 of the inhibitor.

416  
417 **Author Contributions:** Adriana Samide conceived and designed the experiments; Roxana Grecu  
418 and Bogdan Tutunaru performed the electrochemical measurements; Gabriela Eugenia  
419 Iacobescu performed AFM analysis; Adriana Samide, Bogdan Tutunaru and Gabriela Eugenia  
420 Iacobescu wrote the paper. Cristian Tigae and Cezar Spînu contributed with reagents, materials,  
421 analysis tools and software. All authors read the article and critically reviewed it.

422  
423 **Conflicts of Interest:** The authors declare no conflict of interest.

424  
425 **References**

- 427 1. Guo, L.; Obot, I.B.; Zheng, X.; Shen, X.; Qiang, Y.; Kaya, S.; Kaya C. Theoretical insight into  
428 an empirical rule about organic corrosion inhibitors containing nitrogen, oxygen, and  
429 sulfur atoms. *Appl. Surf. Sci.* **2017**, *406*, 301–306.
- 430 2. Samide, A. A pharmaceutical product as corrosion inhibitor for carbon steel in acidic  
431 environments. *J. Environ. Sci. Health A Tox. Hazard. Subst. Environ. Eng.* **2013**, *48*, 159–165.
- 432 3. Aziz, R.J. Study of some drugs as corrosion inhibitors for mild steel in 1M H<sub>2</sub>SO<sub>4</sub> solution.  
433 *Int. J. Curr. Res. Chem. Pharm. Sci.* **2016**, *3*, 1-7.
- 434 4. Samide, A.; Tutunaru, B. Quinine sulfate: a pharmaceutical product as effective corrosion  
435 inhibitor for carbon steel in hydrochloric acid solution. *Cent. Eur. J. Chem.* **2014**, *12*, 901–908.
- 436 5. Samide, A.; Tutunaru, B.; Ionescu, C; Rotaru, P.; Simoiu, L. Aminophylline: thermal  
437 characterization and its inhibitory properties for the carbon steel corrosion in acidic  
438 environment. *J. Therm. Anal. Calorim.* **2014**, *118*, 631–639.
- 439 6. Samide, A.; Tutunaru, B.; Negrilă, C.; Trandafir, I.; Maxut, A. Effect of sulfacetamide on the  
440 corrosion products formed onto carbon steel surface in hydrochloric acid. *Dig. J. Nanomater. Biostruct.* **2011**, *6*, 663–673.
- 441 7. Samide, A.; Tutunaru, B.; Negrilă, C. Corrosion inhibition of carbon steel in hydrochloric  
443 acid solution using a sulfa drug. *Chem. Biochem. Eng. Q.* **2011**, *25*, 299–308.
- 444 8. Samide, A.; Tutunaru, B.; Negrilă, C.; Prunaru, I. Surface analysis of inhibitor film formed  
445 by 4-amino-N-(1,3-thiazol-2-yl) benzene sulfonamide on carbon steel surface in acidic  
446 media. *Spectrosc. Lett.* **2012**, *45*, 55–64.
- 447 9. Gupta, N.K.; Gopal, C.S.A.; Srivastava, V.; Quraishi, M.A. Application of expired drugs in  
448 corrosion inhibition of mild steel. *Int. J. Pharm. Chem. Anal.* **2017**, *4*, 8–12.
- 449 10. Gopiraman, M.; Sakunthala, P.; Kesavan, D.; Alexramani, V.; Kim, I.S.; Sulochana, N. An  
450 investigation of mild carbon steel corrosion inhibition in hydrochloric acid medium by  
451 environment friendly green inhibitors. *J. Coat. Technol. Res.* **2012**, *9*, 15–26.

452 11. Zhu, G.; Hou, J.; Zhu, H.; Qiu, R.; Xu, J. Electrochemical synthesis of poly(3,4-  
453 ethylenedioxythiophene) on stainless steel and its corrosion inhibition performance. *J.  
454 Coat. Technol. Res.* **2013**, *10*, 659-668.

455 12. Palimi, M.J.; Rostami, M.; Mahdavian, M.; Ramezanadeh, B. A study on the corrosion  
456 inhibition properties of silane-modified  $\text{Fe}_2\text{O}_3$  nanoparticle on mild steel and its effect on  
457 the anticorrosion properties of the polyurethane coating. *J. Coat. Technol. Res.* **2015**, *12*, 277-  
458 292.

459 13. Dolabella, L.M.P.; Oliveira, J.G.; Lins, V.; Matencio, T.; Vasconcelos, W.L. Ethanol extract of  
460 propolis as a protective coating for mild steel in chloride media. *J. Coat. Technol. Res.* **2016**,  
461 *13*, 543-555.

462 14. Samide, A.; Tutunaru, B.; Dobrițescu, A.; Ilea, P.; Vladu, A.C.; Tigae, C. Electrochemical  
463 and theoretical study of metronidazole drug as inhibitor for copper corrosion in  
464 hydrochloric acid solution. *Int. J. Electrochem. Sci.* **2016**, *11*, 5520-5534.

465 15. Karthikeyan, S. Drugs/Antibiotics as potential corrosion inhibitors for metals - A review.  
466 *Int. J. ChemTech Res.* **2016**, *9*, 251-259.

467 16. Xhanari, K.; Finsgar, M.; Hrncic, M.K.; Maver, U.; Knez, Z.; Seiti, B. Green corrosion  
468 inhibitors for aluminium and its alloys: a review. *RSC Adv.* **2017**, *7*, 27299-27330.

469 17. Raja, K.; Jeeva, P.A.; Karthikeyan, S. Reduction of hydrogen embrittlement and green  
470 inhibition of stainless steel pipes in acid environment. *Int. J. ChemTech. Res.* **2014-2015**, *7*,  
471 2425-2431.

472 18. Fouada, A.S.; Elmorsi, M.A.; Fayed, T.A.; Hassan, A.F.; Soltan, M. Corrosion inhibitors  
473 based on antibiotic derivatives for protection of carbon steel corrosion in hydrochloric acid  
474 solutions. *Int. J. Adv. Res.* **2014**, *2*, 788-807.

475 19. Chitra, S.; Anand, B. Surface morphological and FTIR spectroscopic information on the  
476 corrosion inhibition of drugs on mild steel in chloride environment. *J. Chem. Pharm. Sci.*  
477 **2017**, *10*, 453-456.

478 20. Zerga, B.; Attayibat, A.; Sfaira, M.; Taleb, M.; Hammouti, B. Ebn Touhami, M.; Radi, S.;  
479 Rais, Z. Effect of some tripodal bipyrazolic compounds on C38 steel corrosion in  
480 hydrochloric acid solution. *J. Appl. Electrochem.* **2010**, *40*, 1575-1582.

481 21. Sobhi, M. Gatifloxacin as corrosion inhibitor for carbon steel in hydrochloric acid solutions.  
482 *Prot. Met. Phys. Chem. Surf.* **2014**, *50*, 825-83.

483 22. Abdallah, M.; AL Jahdaly, B.A. Gentamicin, kanamycin and amikacin drugs as non-toxic  
484 inhibitors for corrosion of aluminium in 1.0 M hydrochloric acid. *Int. J. Electrochem. Sci.*  
485 **2015**, *10*, 9808- 9823.

486 23. Samide, A.; Ilea P.; Vladu, A.C. Metronidazole performance as corrosion inhibitor for  
487 carbon steel, 304L stainless steel and aluminium in hydrochloric acid solution. *Int. J.  
488 Electrochem. Sci.* **2017**, *12*, 5964-5983.

489 24. Bobina, M.; Kellenberger, A.; Millet, J.P.; Muntean, C.; Vaszilcsin, N. Corrosion resistance  
490 of carbon steel in weak acid solutions in the presence of l-histidine as corrosion inhibitor.  
491 *Corros. Sci.* **2013**, *69*, 389-395.

492 25. Nazeer, A.A.; El-Abbas, H.M.; Fouada, A.S. Adsorption and corrosion inhibition behavior  
493 of carbon steel by cefoperazone as eco-friendly inhibitor in HCl. *J. Mater. Eng. Perform.*  
494 **2013**, *22*, 2314-2322.

495 26. Fouda, A.S.; Mostafa, H.A.; El-Abbasy, H.M. Antibacterial drugs as inhibitors for the  
496 corrosion of stainless steel type 304 in HCl solution. *J. Appl. Electrochem.* **2010**, *40*, 163-173.

497 27. Samide, A.; Bibicu, I. Kinetics corrosion process of carbon steel in hydrochloric acid in  
498 absence and presence of 2-(cyclohexylaminomercapto) benzothiazole. *Surf. Interface Anal.*  
499 **2008**, *40*, 944-952.

500 28. Samide, A.; Rotaru, P.; Ionescu, C.; Tutunaru, B.; Moanță, A.; Barragan-Montero, V.  
501 Thermal behaviour and adsorption properties of some benzothiazole derivatives. *J. Therm.*  
502 *Anal. Calorim.* **2014**, *118*, 651-659

503 29. Clarot, I.; Regazzetti, A.; Auzeil, N.; Laadani, F.; Citton, M.; Netter, P.; Nicolas, A. Analysis  
504 of neomycin sulfate and framycetin sulfate by high-performance liquid chromatography  
505 using evaporative light scattering detection. *J. Chromatogr. A.* **2005**, *1087*, 236-244.

506 30. Hanko, V.P.; Rohrer, J.S. Determination of neomycin sulfate and impurities using high-  
507 performance anion-exchange chromatography with integrated pulsed amperometric  
508 detection. *J. Pharmaceut. Biomed.* **2007**, *43*, 131-141.

509 31. Abraha, A.; Gholap, A.V.; Belay, A. Study Self-association, Optical Transition Properties  
510 and Thermodynamic Properties of Neomycin Sulfate Using UV-Visible Spectroscopy. *Int.*  
511 *J. Biophys.* **2016**, *6*, 16-20.

512 32. Geetha, M.B.; Rajendran, S. Synergistic Inhibition of Corrosion of Mild Steel in Sulphuric  
513 acid by New Ternary System. *Der Pharma Chemica* **2016**, *8*, 194-201.

514 33. Samide, A.; Iacobescu, G.E.; Tutunaru, B.; Tigae, C. Electrochemical and AFM Study of  
515 Inhibitory Properties of Thin Film Formed by Tartrazine Food Additive on 304L Stainless  
516 Steel in Saline Solution. *Int. J. Electrochem. Sci.* **2017**, *12*, 2088-2101.

517 34. Samide, A.; Tutunaru, B. Eurovanillin thermal behaviour and its inhibitory properties on  
518 carbon steel corrosion in weakly acidic environments. *J. Therm. Anal. Calorim.* **2017**, *127*,  
519 863-870.

520 35. Abdel Ghany, N.A.; El-Shenawy, A.E.; Hussien, W.A.M. The Inhibitive effect of some  
521 amino acids on the corrosion behaviour of 316L stainless steel in sulfuric acid solution.  
522 *Mod. Appl. Sci.* **2011**, *5*, 19-29.

523